Supplement of Nat. Hazards Earth Syst. Sci., 19, 1839–1864, 2019
https://doi.org/10.5194/nhess-19-1839-2019-supplement

Natural Hazards and Earth System Sciences
Open Access

Supplement of

The impact of lightning and radar reflectivity factor data assimilation on the very short-term rainfall forecasts of RAMS@ISAC: application to two case studies in Italy

Stefano Federico et al.

Correspondence to: Stefano Federico (s.federico@isac.cnr.it)

S1 Introduction

In this supplemental material, we discuss several sensitivity tests of lightning and radar reflectivity factor data assimilation. In particular: a) the contribution of data assimilation to the evolution of total water for each source of data is considered in Section S2; b) the sensitivity of rainfall VSF to the formulation of lightning data assimilation is discussed in Section S3; c) the sensitivity of rainfall VSF to two specific aspects of radar reflectivity factor data assimilation is considered in Section S4; d) the sensitivity of rainfall VSF to RAMS@ISAC setting is discussed in Section S5.

Section S6 shows the impact of lightning data assimilation for a case study well predicted by the control forecast, which doesn't assimilate neither lightning nor radar reflectivity factor. A different representation of the Figures 15-17 of the paper is provided in Section S7. The form of the forward radar operator is provided in Section S8. Conclusions are given in section S9. Table 1 shows the list of the simulations discussed in this supplemental material.

S2 Evolution of total water

Because both lightning data assimilation and radar reflectivity factor data assimilation adjust the water vapour mixing ratio (q_v), it is interesting to evaluate the contribution of each data source to the q_v adjustment including in this evaluation the assimilation phase (0-6 h).

Fierro et al. (2015) used the total water substance mass (accumulated precipitation + total hydrometeors and water vapour mass) to quantify the impact of lightning data assimilation by nudging. Here we use a similar approach. More specifically, we consider the forecasted accumulated precipitation and the total hydrometeors and water vapour mass averaged over the grid columns. Moreover, we averaged all VSFs for Serano and Livorno. Figure S1a shows the evolution of accumulated precipitation forecast, while Figure S1b shows the evolution of hydrometeors plus water vapour mass forecast.

Figures S1a and S1b show that flashes add less water vapour compared to radar reflectivity factor data assimilation and, of course, RADLI has the largest impact. In particular, the total water mass added to the background at the end of VSF is 2.5%, 5.7% and 7.4% of the background value for LIGHT, RAD and RADLI, respectively.

Interestingly, the total water mass added by RADLI to the background is less than the sum of the total water masses added by RAD and LIGHT. This happens because RAMS-3DVar adds water to the background limiting the impact of nudging during the simulation and vice-versa.

Accumulated precipitation accounts for the largest part of the water mass added to the simulation, similarly to Fierro et al. (2015). At the end of the assimilation phase (6h), the evolution of the hydrometeors plus water vapour mass converges towards the background as boundary conditions propagate into the domain.

S3 Sensitivity to nudging formulation

As stated in Section 3.2 of the paper, the application of the Fierro et al. (2012) method to RAMS@ISAC is not straightforward. Furthermore, the optimal setting of the coefficients of Eqn. (1) (see the paper for the expression of the equation) depends on the case study. For these reasons, it is important to evaluate the sensitivity of the results to the nudging formulation. For this purpose, we show the variability of ETS and POD scores with A and B coefficients of Eqn. (1). The scores are computed considering all VSF of the two case studies for different configurations: A_76 has the coefficients A=0.76 and B=0.25; LIGHT has A=0.86 and B=0.15 (default setting), SAT has A=1.01 and B=0; RADLI has A=0.86 and B=0.15 (default setting).

Scores are computed for RAMS@ISAC second domain considering the nearest neighbourhood rainfall for all VSF of Serano and Livorno. ETS score (Figure S2a) shows that all configurations assimilating either lightning or radar reflectivity factor or both observations improve the forecast for all thresholds. RADLI has the best ETS for rainfall intensity larger than 32 mm/3h in agreement with the results of the three VSF discussed in the paper.

Simulations assimilating lightning perform better than simulations assimilating radar reflectivity factor for thresholds lower than 32 mm/3h because they have less false alarms (not shown). A_76 has the worst score among all simulations assimilating lightning. The comparison between LIGHT and SAT shows mixed results: SAT performs better up to 32 mm/3h, while LIGHT is better for higher thresholds. This behaviour is confirmed by the POD (Figure S2b). A visual inspection of the model output reveals that, for high rainfall intensities, SAT generates spurious convection in some areas while misses convection in other areas that are correctly forecast by LIGHT.

Lynn et al. (2015) implemented a method suggested by Fierro et al. (2012) to suppress spurious convection in WRF (Weather Research and Forecasting Model). This method compares the lightning forecast during the assimilation period with observations to filter out spurious convection. The application of the methodology on 10 July 2013 improved the forecast of the squall line from Texas to Iowa, which was the focus of the forecast on that day; however, the application of the method to 19 and 21 March 2012 over the CONUS gave mixed results, improving the forecast in the first 6h and worsening it in the following hours.

The implementation of this method could be used in RAMS@ISAC in future applications of the nudging scheme, to suppress spurious convection.

It is finally noted that RAD and RADLI have high POD values for all thresholds, nevertheless their ETS is below that of LIGHT and SAT for rainfall intensities up to 32 mm/3h for RADLI and up to 42 mm/3h for RAD. This behaviour is caused by the larger number of false alarms in simulations assimilating radar reflectivity factor compared to those assimilating lightning. This result shows again that RAD and RADLI configurations have a wet bias. In particular, the frequency bias of RAD and RADLI configuration is about 3 for thresholds between 20 and 40 mm/3h.

S4 Sensitivity to radar formulation

In this section sensitivity tests involving two different settings of radar reflectivity factor data assimilation are performed: a) observation error (1 to 3 dBz for the default setting); b) the shape of the area used for computing the relative humidity pseudo-profiles.

We limit the discussion to the Livorno case, which is the most intense between the two events considered in the paper.

For the sensitivity to the radar reflectivity factor observation error, it is important to note that this error is used when computing the relative humidity pseudo profiles and not in RAMS-3DVar, where the NMC method (Parrish and Derber, 1992) is used. Because the model missed the event, the assimilation of radar reflectivity factor caused a model wetting. This humidity, however, is mainly added for the following reason: RAMS@ISAC doesn't simulate any reflectivity factor while the radars show positive values of reflectivity factor (for example most of the relative humidity added over central Italy and over Sardinia is produced by this occurrence). When this happens, the model is saturated above the LCL where the observed reflectivity factor is greater than zero and the error of radar observations is not used (the error of radar reflectivity factor is used for computing pseudo-profiles, which are used when the background provides already a good forecast of reflectivity factor). Although the error of radar reflectivity factor observations is important and a too small value could make the method too sensitive to radar observation, especially when combined with a pure sampling of the radar data as in our setting, this problem is less important for the case studies considered in this paper because they are missed by RAMS@ISAC.

The shape of the area used for computing relative humidity pseudo-profiles for the radar data assimilation is a square in this paper, according to Caumont et al. (2010). However, a circle is also a good choice because it considers grid points equidistant from the centre along the circumference. The impact of this geometry, however, is expected negligible because pseudo profiles are less important in the data assimilation of the cases considered in this paper, as explained above.

Figure S3 shows the precipitation forecast between 06 and 09 UTC on 10 September 2017 by the VSF assimilating radar with the default setting (RAD), by the VSF assimilating radar reflectivity factor with and error increased by 5 compared to the RAD simulation (in this case the radar reflectivity factor error varies between 5dBz and 15 dBz), and by the VSF using a circle with 50 km diameter for computing relative humidity pseudo-profiles (CIRC). There are small differences at the local scale but the precipitation VSF are very similar. The POD and ETS scores computed for the ten VSF of the Livorno case (Figure S4) confirm this result. Differences among RAD, RAD5 and CIRC are very small and increasing the radar reflectivity factor error or changing the shape of the area used for computing relative humidity pseudo-profiles has a minor impact on the rainfall VSF for the Livorno case study.

S5 Sensitivity to model formulation

In this section, we study the sensitivity of the rainfall VSF for the Livorno case to two aspects of the model formulation: a) updating initial (IC) and boundary conditions (BC) (RLAA simulation); b) increasing the number of vertical levels from 36 to 42 (simulations CTRL42 and ANL42).

The RLAA simulation uses updated IC/BC that assimilates new data as they become available. IC and BC for the R4 domain are interpolated from the output of R10 domain, and, in order to update IC and BC, analyses are done for the R10 domain.

These analyses assimilate radar reflectivity factor every one-hour by RAMS-3DVar and lightning by nudging, similarly to R4 domain. The background error matrix for the RAMS-3DVar for the R10 domain is obtained applying the NMC method to the HyMeX-SOP1 period.

Ten VSF are run with R10. Each VSF lasts 9h and data assimilation is performed for the first six-hours. Those VSF are used to create IC/BC for the RLAA simulations.

The impact of updating IC and BC for the R4 VSF is expected to be small for the setting of this paper. The impact of BC is presumed low because radar and lightning observations are inside the R4 domain.

The impact of updating IC is also expected to be low because even if IC are substantially changed by the radar reflectivity factor data assimilation over the R10 domain, when the VSF starts on R4 an analysis is made assimilating radar reflectivity factor on R4 domain. So, if the IC for this VSF forecast on R4 are interpolated from the R10 background (setting of the paper) the innovations given by the analysis over the R4 at initial time are large; if IC are interpolated from an R10 analysis (RLAA setting), the innovations of the first analysis over the R4 domain are small, because IC already take into account for the radar reflectivity factor data assimilation. However, the final result is similar in both cases.

These considerations are confirmed by the results for the Livorno case. In particular, POD and ETS for the RLAA simulation are similar to those of RADLI forecast (Figure S5). POD for RLAA has slightly better performance (2-3%) compared to RADLI for specific thresholds, showing a positive impact of updating IC/BC as new data become available, nevertheless the impact is small and a detailed study, considering more cases, is needed to draw conclusions about this improvement.

It is important to note, however, that if the observations are close to the edge of the domain or cross the domain, the impact of BC is expected to be more important than that found in this paper.

To show the sensitivity of the results to the number of vertical levels we consider the simulation of the Livorno case using RAMS@ISAC with 42 levels (hereafter R_42) instead of 36 levels (R_36). This choice is motivated by the fact that RAMS@ISAC with 42 levels will be operational starting from September 2019. R_42 has a higher vertical resolution than R_36. The complete list of levels used in R_36 and R_42 is reported in Table S2.

We simulated the Livorno case using R_42 assimilating lightning and radar reflectivity factor data (ANL42). This experiment needed a control run using R_42 (CTRL42).

It is important to note that the background error matrix for RAMS@ISAC with 42 levels was interpolated/extrapolated from that of RAMS@ISAC with 36 levels (the application of the NMC method would require the simulation of the entire HyMeX-SOP1 period using R_42). While we believe that this choice is reasonable for this experiment, it could result in non-optimal adjustments given by RAMS-3DVar.

Figure S6a and S6b show, respectively, the rainfall VSF for CTRL and CTRL42 between 06 and 09 UTC on 10 September 2017, when the storm was active mainly over Lazio (Section 4.2.2 of the paper).

The increasing of the number of levels did not result in an improvement of the precipitation forecast over Lazio. There are, however, differences at the local scale especially over Tuscany and NE of Italy.

It is also notable the higher rainfall between Corsica and Italian peninsula for CTRL42. This feature is systematic for all VSF of the Livorno case and it is likely caused by a better representation of the interaction between the air-masses and the complex orography of Corsica in R_42. Figure S6c and S6d show the rainfall VSF between 06 and 09 UTC given by RADLI and ANL42. Differences between the two forecasts are small and at the local scale.

POD and ETS scores for R_42 considering the ten VSF of the Livorno case over the R4 domain are shown in Figure S5 for both CTRL42 and ANL42. The POD of CTRL42 is higher than that of CTRL but the improvement is small (2-3%). The POD of ANL42 is slightly worse than that of RADLI. Difference between RADLI and ANL42 could be the result of the specific case considered or a consequence of the non-optimal setting of RAMS-3DVar for ANL42.

The results for ETS score, which penalizes false alarms, show less differences between R_36 and R_42 settings.

Thus, the results of the experiment using 42 vertical levels in RAMS@ISAC are similar to those using 36 levels and show again the crucial role of lightning and radar reflectivity factor data assimilation for the successful forecast of the Livorno case.

S6 A well predicted case study

In this section, we show the impact of data assimilation for a case well predicted by the CTRL simulation, without lightning or radar reflectivity factor data assimilation. To keep the discussion concise, we limit the analysis to lightning data assimilation.

The case study occurred on 5 November 2017 and was chosen because it is similar to Serano and Livorno from a synoptic perspective. In particular, the storm was caused by a trough extending from northern Europe towards the Mediterranean. The interaction between the trough and the Alpine orography caused a low pressure over the Gulf of Genova (not shown). The storm propagated towards SE and, in these conditions, humid and unstable air masses were advected from the Tyrrhenian Sea towards the Italian mainland.

The convection developed over the Tyrrhenian Sea and over the Italian peninsula (especially on its western side), as shown by the lightning density observation on this day (Figure S7): more than 100.000 flashes were detected for this intense event. Moderate to heavy rainfall occurred in several parts of Italy. In particular, between 12 and 15 UTC intense precipitation fell around Rome (Figure S8a) with values greater than 50 mm/3h reported by several raingauges. Some areas of the city were flooded, and problems occurred in local transportation system in outdoor activities.

The intense precipitation over Rome was well predicted by the VSF of the CTRL forecast (Figure S8b), even if there is a shift to the north of the precipitation pattern (15-20 km). The intense precipitation over NE of Italy and the rainfall over Liguria and Tuscany were also well predicted.

Figure S8c shows the rainfall VSF for LIGHT simulation. The VSF follows a 6 h assimilation phase (6-12 UTC for this specific VSF), when more than 34000 flashes are assimilated in RAMS@ISAC following the method of Fierro et al. (2012). LIGHT rainfall VSF is similar to CTRL and lightning data assimilation has a lower impact on the rainfall VSF compared to Livorno or Serano case studies. Of course, considering the high number of assimilated lightning, there are differences between CTRL and LIGHT rainfall VSF, but they do not change substantially the forecast given by CTRL. Rainfall simulated by LIGHT is shifted to the south (15-20 km) compared to CTRL, in better agreement with observations. However, LIGHT VSF overestimates the area of intense precipitation (>30-40 mm/3h).

To discuss more in detail the lower impact of lightning data assimilation for the 5 November case study compared to Serano and Livorno, we consider the vertical cross section of relative humidity at 42°N (Figure S9a) and at the end of the assimilation phase (12 UTC). The vertical section shows very humid layers (relative humidity >92.5%). One of these layers is over the Tyrrhenian Sea (11 °E -12.5 °E). Considering that 0 °C and -25 °C isotherms heights are about 2500 m and 7000 m, it is expected a low impact of lightning data assimilation for this layer. This is confirmed by Figure S9b, which shows the same cross section of Figure S9a for LIGHT simulation. The humid layer over the Tyrrhenian Sea is slightly wider for LIGHT, but differences are overall small. The analyses of other fields, as the averaged specific humidity between 3 and 10 km, also show the low impact of lightning data assimilation for this VSF.

In conclusion, the analysis of the 5 November 2017 event, shows that the impact of lightning data assimilation is much lower when the CTRL VSF has a good performance. Interestingly, lightning data assimilation improves the rainfall forecast at the local scale even for well predicted events, while overestimates the precipitation. This is the main drawback of lightning data assimilation in RAMS@ISAC.

S7 New plots

Figures S10-S12 show a different representation of the Figures 15-17 of the paper. In particular, we show the rainfall predicted by RAMS@ISAC for the three VSF considered in the paper interpolated at the stations' positions. From Figure S12, in particular, the overestimation of the precipitation field given by both RAD and RADLI is apparent (see also Section 4.2.2 in the paper).

S8 Forward radar operator

In the method of Caumont et al. (2010) there is the need to simulate reflectivity factor (in dBz) from the model output. To compute the reflectivity factor we use the forward operator of Stoelinga used in the RIP (Read/Interpolate/Plot) software of WRF (https://dtcenter.org/wrf-nmm/users/OnLineTutorial/NMM/RIP/index.php, last access 03 March 2019).

The software assumes Rayleigh scattering regime (at C-band this assumption can be considered as valid for light to moderate rain) and includes the contribution of rain, snow and graupel. Particles are assumed spherical with constant density ($\rho_r = \rho_l$=1000 kg/m^3; ρ_s=100 kg/m^3; ρ_g =400 kg/m^3; *r* stands for rain, *l* for liquid, *s* for snow and *g* for graupel).

The size distribution of the hydrometeors follows an exponential distribution given by:

$$N(D) = N_0 e^{-\lambda D} \tag{S1}$$

Where N_0 is constant for each hydrometeor (N_{0r}=8x10^6 m^{-4},N_{0s}=2x10^7 m^{-4},N_{0g}=4x10^6 m^{-4}).

Using these assumptions, the reflectivity factor for rain Z_{er}, which is the sixth moment of the size distribution, is given by:

$$Z_{er} = \Gamma(7) N_{0r} \lambda^{-7} \tag{S2}$$

where Γ is the gamma function. The shape factor λ depends on the simulated mixing ratio (q_r) and it is given by:

$$\lambda_r = \left(\frac{\pi N_{0r} \rho_r}{\rho_a q_r} \right)^{1/4} \tag{S3}$$

where ρ_a is the density of dry air.

In the case of snow, the reflectivity factor Z_{es} is given by:

$$Z_{es} = \Gamma(7) N_{0s} \lambda^{-7} \left(\frac{\rho_s}{\rho_l} \right)^2 \alpha \tag{S4}$$

where α=0.224. The reflectivity factor for graupel is the same as (S4) with N_{0g} replacing N_{0s}, and ρ_g replacing ρ_s . Since the reflectivity factor, when expressed in mm^6/m^3, is an additive quantity, the contributions of rain, snow, and graupel can be added to obtain the reflectivity factor:

$$Z_{etot}=Z_{er}+Z_{eg}+Z_{es}$$

and in dBz is given by:

$$Z_e(dBz)=10\ log(Z_{etot}\ (\text{in mm}^6\text{m}^{-3}))$$

S.9 Conclusions

The analysis of the evolution of the total water mass shows that flashes add less water vapour to the VSF than radar reflectivity factor data assimilation. This, however, even if in agreement with other studies (Fierro et al., 2016) could be a result of the specific case studies.

The sensitivity of the rainfall VSF to the nudging formulation for lightning data assimilation shows that reducing the amount of water vapour added to RAMS@ISAC compared to the default set-up has a worse impact on ETS and POD. Nevertheless, assuming saturation (SAT) for grid points where lightning is observed gave mixed results. Spurious convection was generated in the SAT configuration, which decreased the performance of the model for thresholds larger than 34 mm/3h. A method proposed by Fierro et al. (2012) and used in Lynn et al. (2015) could be used in future implementations of the nudging scheme to suppress spurious convection.

Increasing the radar reflectivity factor error (RAD5) or changing the shape of the area used to compute pseudo-profiles (CIRC) had a minor impact on the rainfall VSF. Furthermore, updating IC/BC as new data are available (RLAA) and increasing the number of vertical levels in RAMS@ISAC (CTRL42, ANL42) gave minor changes to the rainfall VSF. Therefore, the sensitivity tests generalize the findings of the paper.

Finally, the results for a case study well predicted by the background show a limited impact of lightning data assimilation.

References

Caumont, O., Ducrocq, V., Wattrelot, E., Jaubert, G., and Pradier-Vabre, S.: 1D+3DVar assimilation 753 of radar reflectivity data: a proof of concept, Tellus A: Dynamic Meteorology and 754 Oceanography, 62:2, 173-187, https://www.tandfonline.com/doi/abs/10.1111/j.1600- 755 0870.2009.00430.x, 2010.

Fierro, A. O., Mansell, E., Ziegler, C., and MacGorman, D.: Application of a lightning data assimilation technique in the WRFARW model at cloud-resolving scales for the tornado outbreak of 24 May 2011, Mon. Weather Rev., 140, 2609–2627, 2012.

Fierro, A. O., A. J. Clark, E. R. Mansell, D. R. MacGorman, S. Dembek, and C. Ziegler: Impact of storm-scale lightning data assimilation on WRF-ARW precipitation forecasts during the 2013 warm season over the contiguous United States. Mon. Wea. Rev., 143, 757–777, 2015. doi:https://doi.org/10.1175/MWR-D-14-00183.1.

Fierro, A.O., Gao, l., Ziegler, C. L., Calhoun, K. M., Mansell, E. R., and MacGorman, D. R.: Assimilation of Flash Extent Data in the Variational Framework at Convection-Allowing Scales: Proof-of-Concept and Evaluation for the Short-Term Forecast of the 24 May 2011 Tornado Outbreak. Mon. Wea. Rev., 144, 4373–4393,https://doi.org/10.1175/MWR-D-16-0053.1, 2016.

Lynn, B. H., G. Kelman, and G. Ellrod, 2015: An evaluation of the efficacy of using observed lightning to improve convective lightning forecasts. Wea. Forecasting, 30, 405-423 doi:10.1175/ WAF-D-13-00028.1.

Parrish, D.F., and Derber, J.C.: The National Meteorological Center's Spectral Statistical Interpolation analysis system, Monthly Weather Review, 120, 1747-1763, 1992.

Table S1: Simulations considered in this supplement material.

Experiment	Description	Data assimilated	Model variable impacted	Note
CTRL	Control run	None	None	/
RAD	RADAR data assimilation	Reflectivity factor CAPPI (RAMS-3DVar)	Water vapour mixing ratio	/
LIGHT	Lightning data assimilation (A=0.86; B=0.15 in Eqn (1))	Lightning density (nudging)	Water vapour mixing ratio	/
RADLI	RADAR + lightning data assimilation (A=0.86; B=0.15 in Eqn (1))	Reflectivity factor CAPPI (RAMS-3DVar) + Lightning density (nudging)	Water vapour mixing ratio	/
A_76	Lightning data assimilation (A=0.76; B=0.25 in Eqn (1))	Lightning density (nudging)	Water vapour mixing ratio	/
SAT	Lightning data assimilation (A=1.01; B=0. in Eqn (1))	Lightning density (nudging)	Water vapour mixing ratio	/
RAD5	RADAR data assimilation.	Reflectivity factor CAPPI (RAMS-3DVar)	Water vapour mixing ratio	As RAD simulation but with the

				error of radar reflectivity factor increased by 5.
CIRC	RADAR data assimilation	Reflectivity factor CAPPI (RAMS-3DVar)	Water vapour mixing ratio	As RAD but with a circular shape to compute relative humidity pseudo-profiles
RLAA	RADAR + lightning data assimilation (A=0.86; B=0.15 in Eqn (1)).	Reflectivity factor CAPPI (RAMS-3DVar) + Lightning density (nudging)	Water vapour mixing ratio	As RADLI but with updated IC/BC as new data are available
CTRL42	Control run	None	None	As CTRL simulation but using 42 vertical levels
ANL42	RADAR + lightning data assimilation (A=0.86; B=0.15 in Eqn (1))	Reflectivity factor CAPPI (RAMS-3DVar) + Lightning density (nudging)	Water vapour mixing ratio	As RADLI simulation but using 42 vertical levels

Table S2: Vertical levels of RAMS@ISAC with 36 levels (default setting, R_36) and RAMS@ISAC with 42 levels (R_42).

RAMS@ISAC CONFIGURATION	LEVEL (m)

R_36	0, 50, 108, 174, 250, 337, 438, 553, 686, 839, 1015, 1217, 1450, 1718, 2025, 2379, 2786, 3254, 3792, 4411, 5122, 5941, 6882, 7964, 9164, 10364, 11563, 12764, 13964, 15164, 16364, 17564, 18764, 19964, 21164, 22364
R_42	0, 50, 106, 167, 235, 311, 396, 489, 593, 708, 836, 978, 1136, 1311, 1505, 1720, 1959, 2225, 2520, 2847, 3210, 3613, 4061, 4557, 5109, 5721, 6400, 7154, 7991, 8920, 9951, 1096, 12296, 13496, 14696, 15896, 17096, 18296, 19496, 20696, 21896, 23096

a)

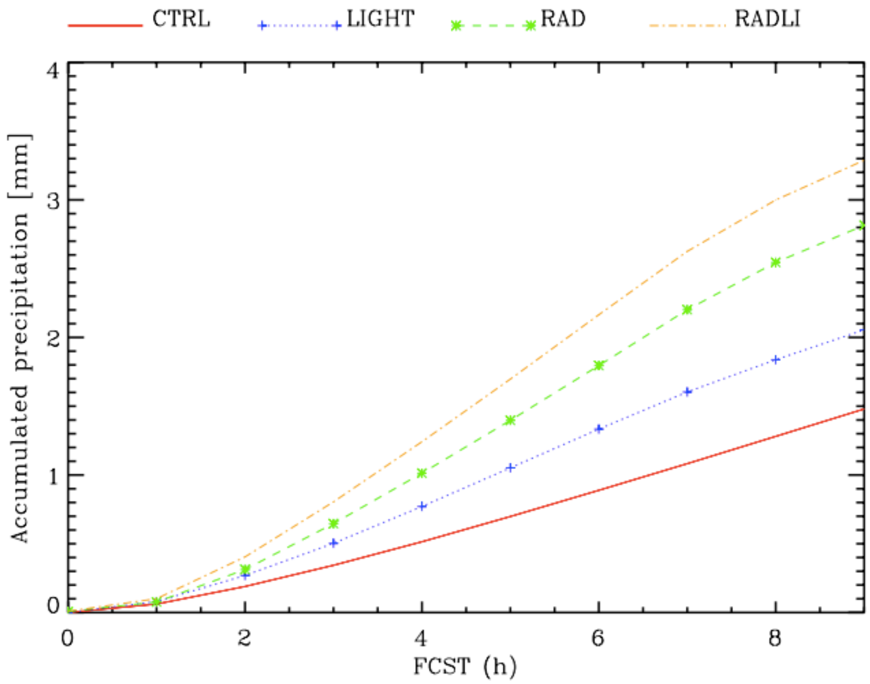

b)

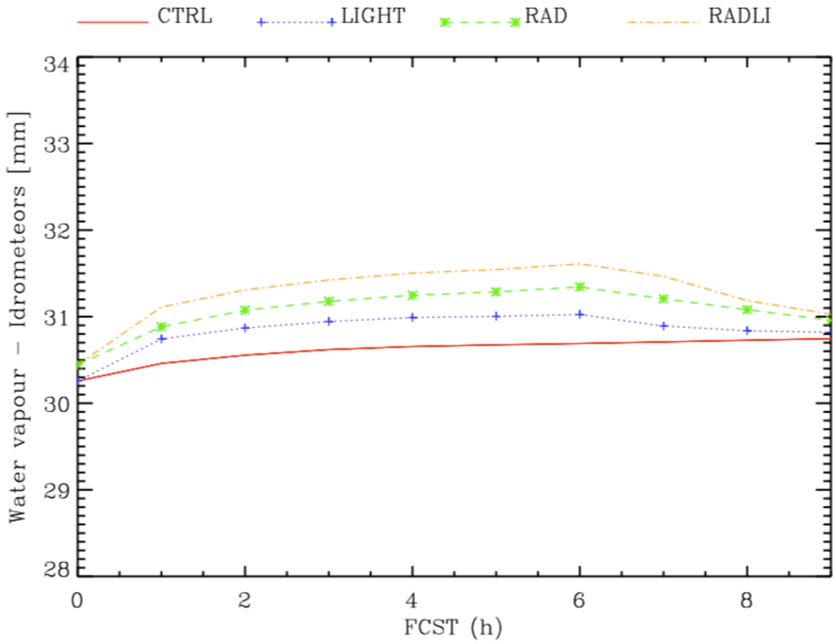

Figure S1: a) Evolution of accumulated precipitation for different model configurations and for all forecast hours; b) as in a) for the hydrometeors plus water vapour mass per unit area. All quantities are expressed in [mm] and are averaged over the number of grid columns.

a)

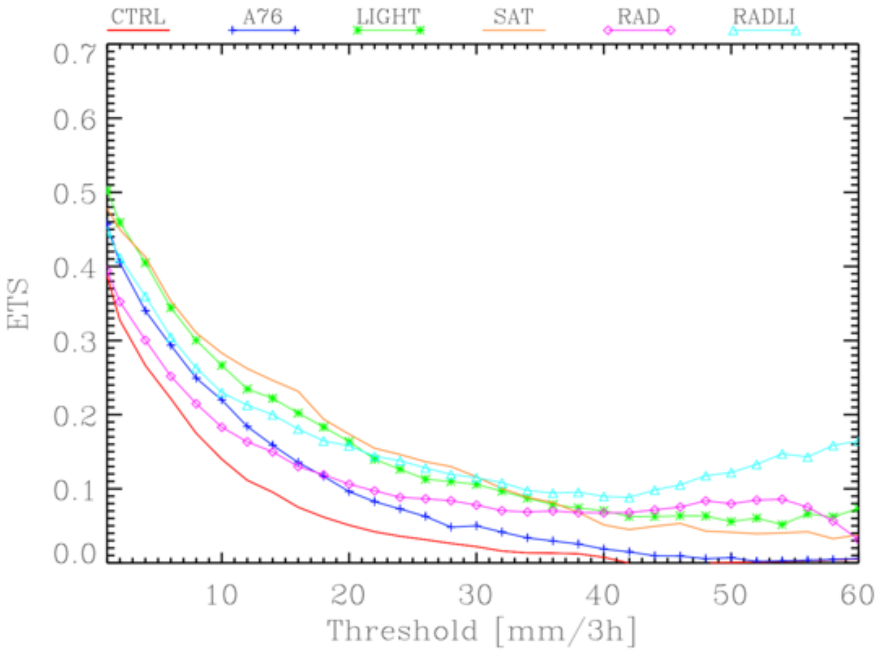

b)

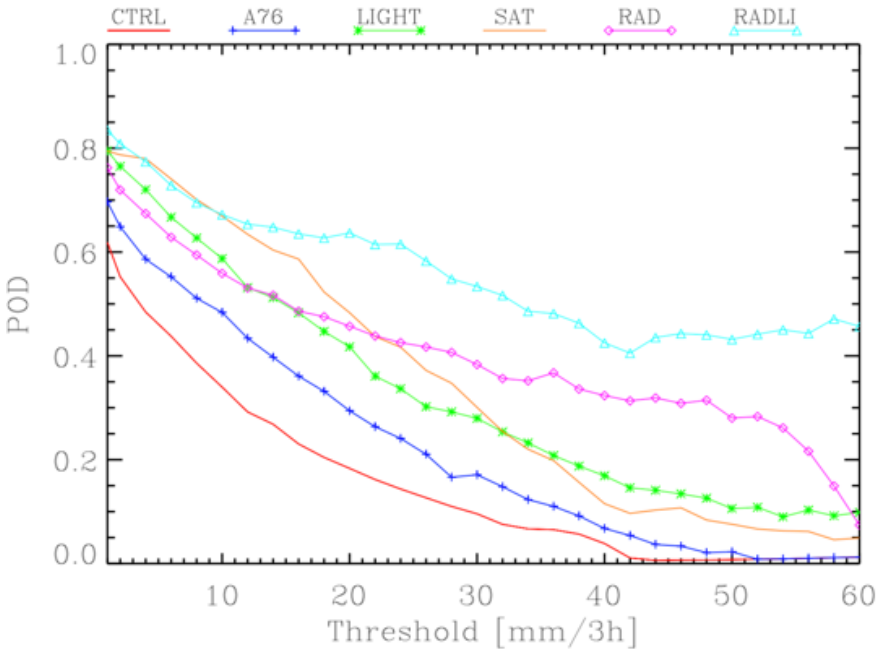

Figure S2: a) ETS score for all VSF considered in this paper; b) as in a) for the POD score. Scores are computed for the R4 domain considering all VSF for Livorno and Serano cases. Scores are computed for the nearest neighbourhood and for the thresholds: 1mm/3h, 2mm/3h and then every 2 mm/3h up to 60 mm/3h.

a)

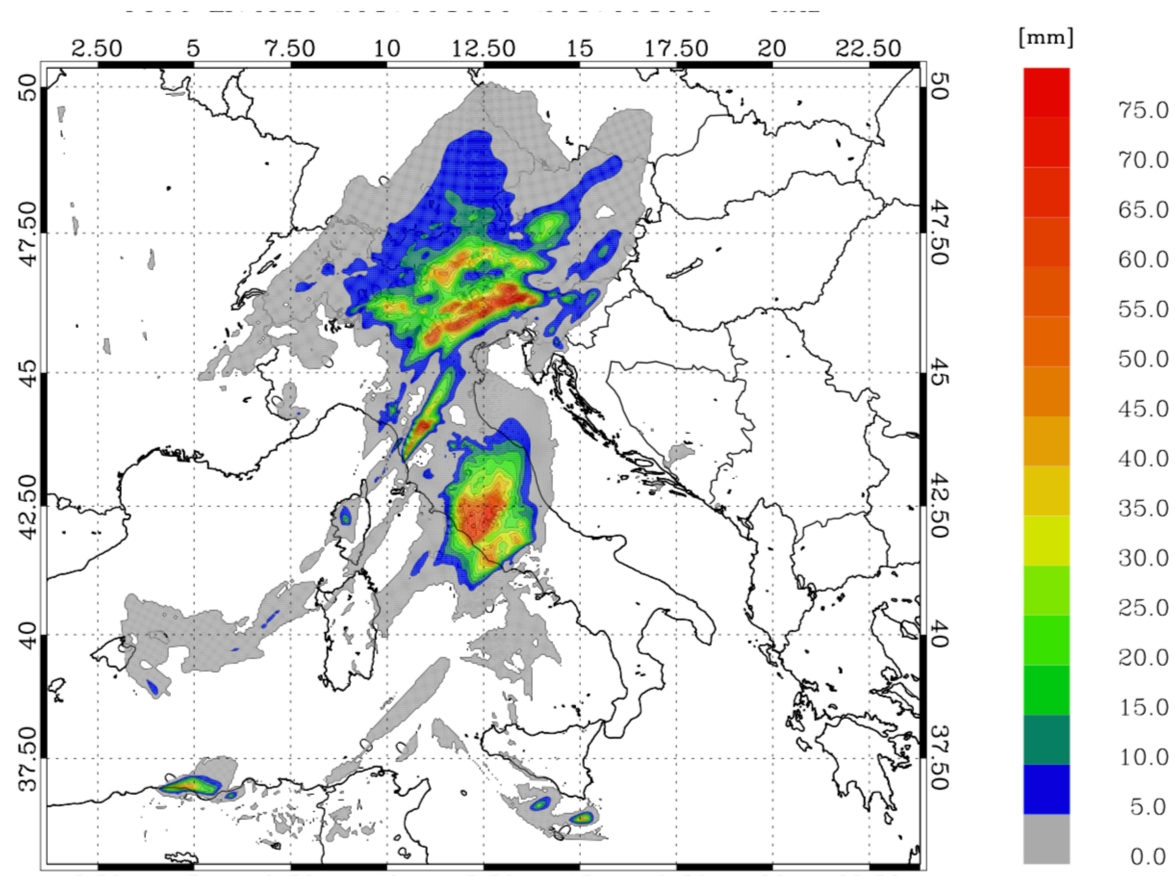
[mm]
75.0
70.0
65.0
60.0
55.0
50.0
45.0
40.0
35.0
30.0
25.0
20.0
15.0
10.0
5.0
0.0
2.50
5
7.50
10
12.50
15
17.50
20
22.50
50
47.50
45
42.50
40
37.50

b)

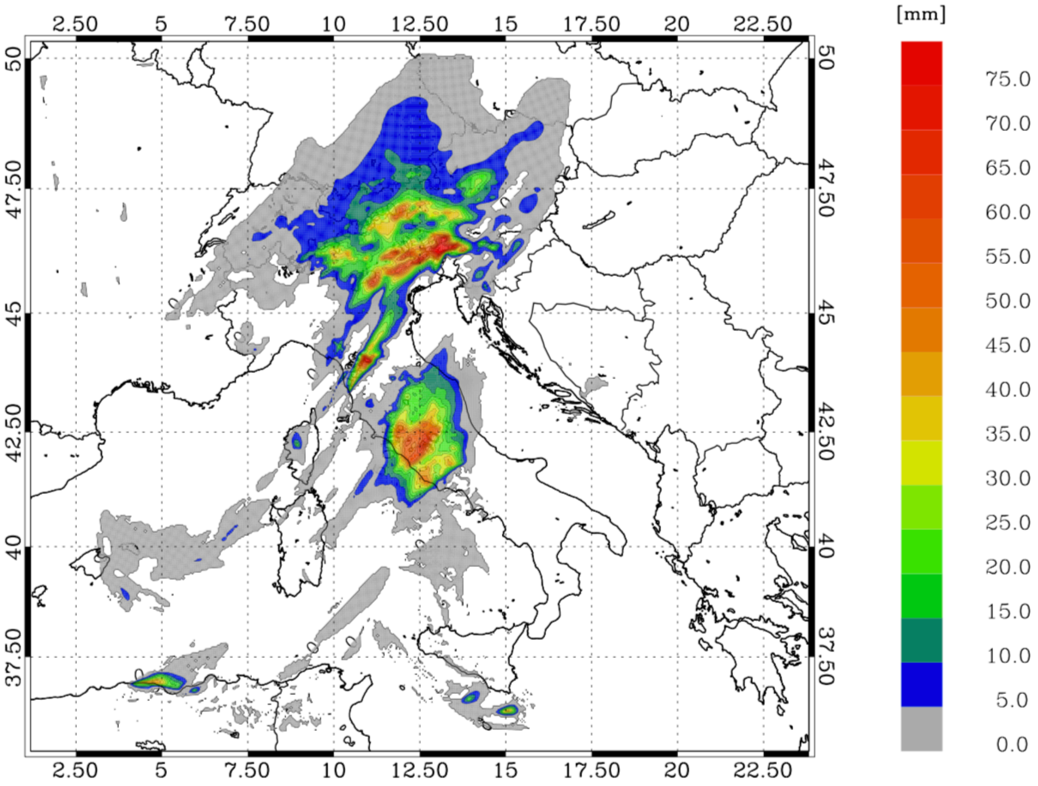
2.50 5 7.50 10 12.50 15 17.50 20 22.50
50 47.50 45 42.50 40 37.50
[mm]
75.0
70.0
65.0
60.0
55.0
50.0
45.0
40.0
35.0
30.0
25.0
20.0
15.0
10.0
5.0
0.0

c)

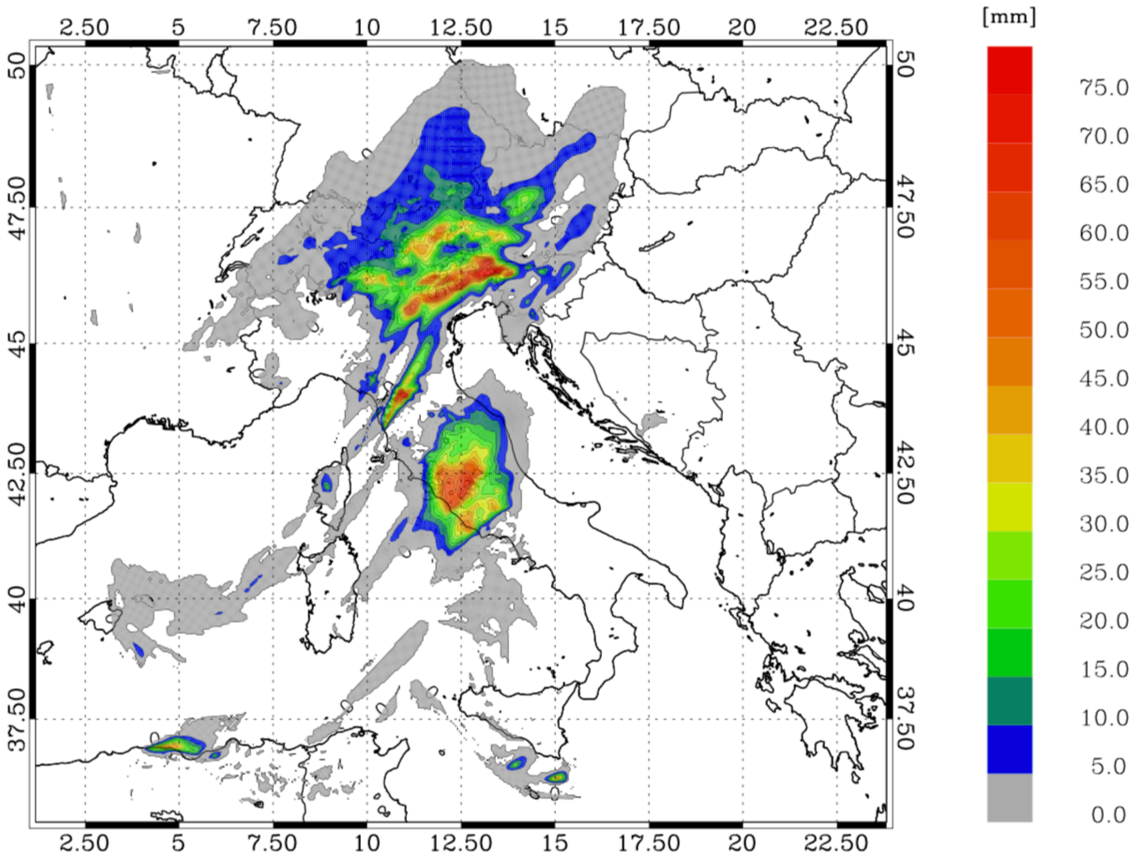

Figure S3: a) rainfall VSF between 06 and 09 UTC on 10 September for RAD; b) as in a) for RAD5; c) as in a) for CIRC.

a)

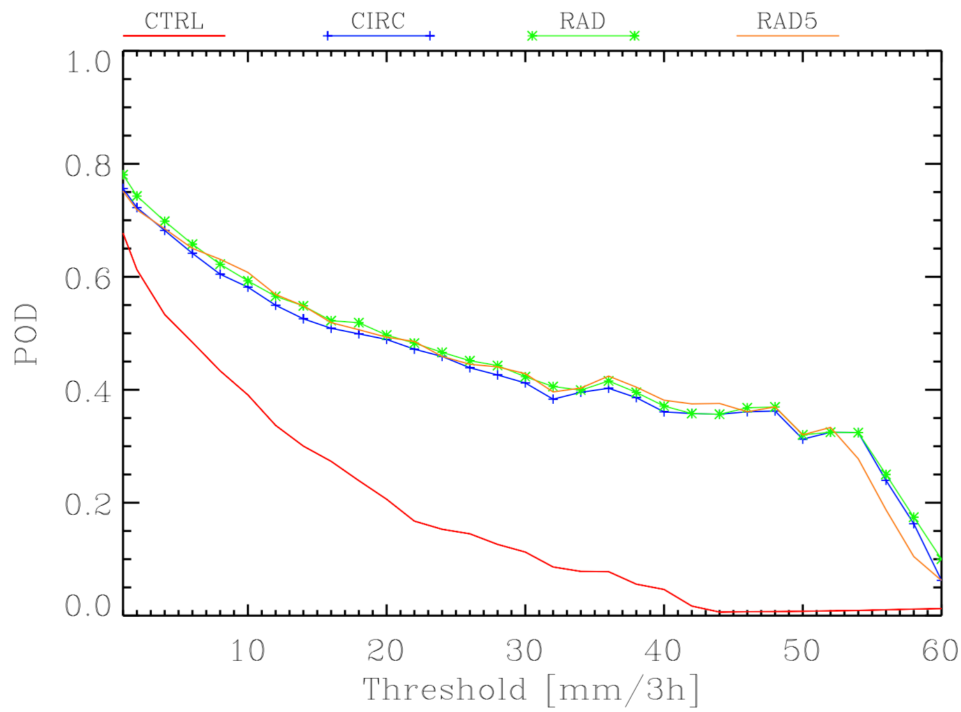

b)

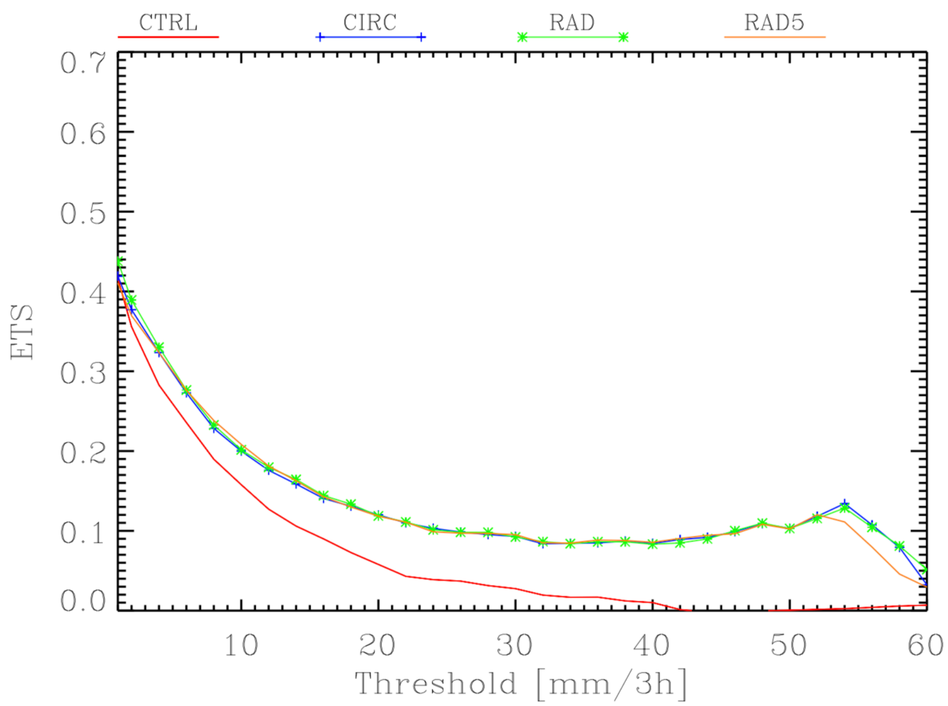

Figure S4: a) POD score for Livorno; b) as in a) for ETS score. CTRL is the control simulation, RAD is the simulation assimilating radar reflectivity factor, RAD5 is the simulation with a reflectivity factor error five times that of RAD; CIRC is the simulation using a circle for computing relative humidity pseudo-profiles. Scores are computed for the R4 domain considering the ten VSF of the Livorno case. Scores are computed for the nearest neighbourhood and for the threshold of: 1mm/3h, 2mm/3h and then every 2 mm/3h up to 60 mm/3h, considering the R4 domain and the ten VSF of the Livorno case.

a)

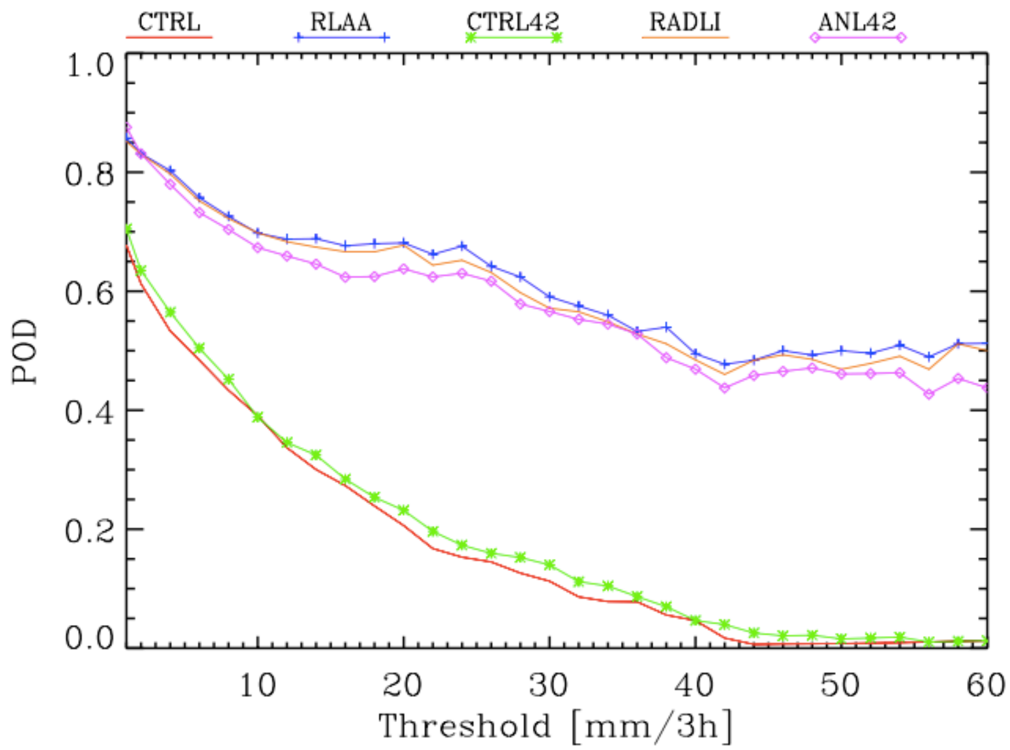

b)

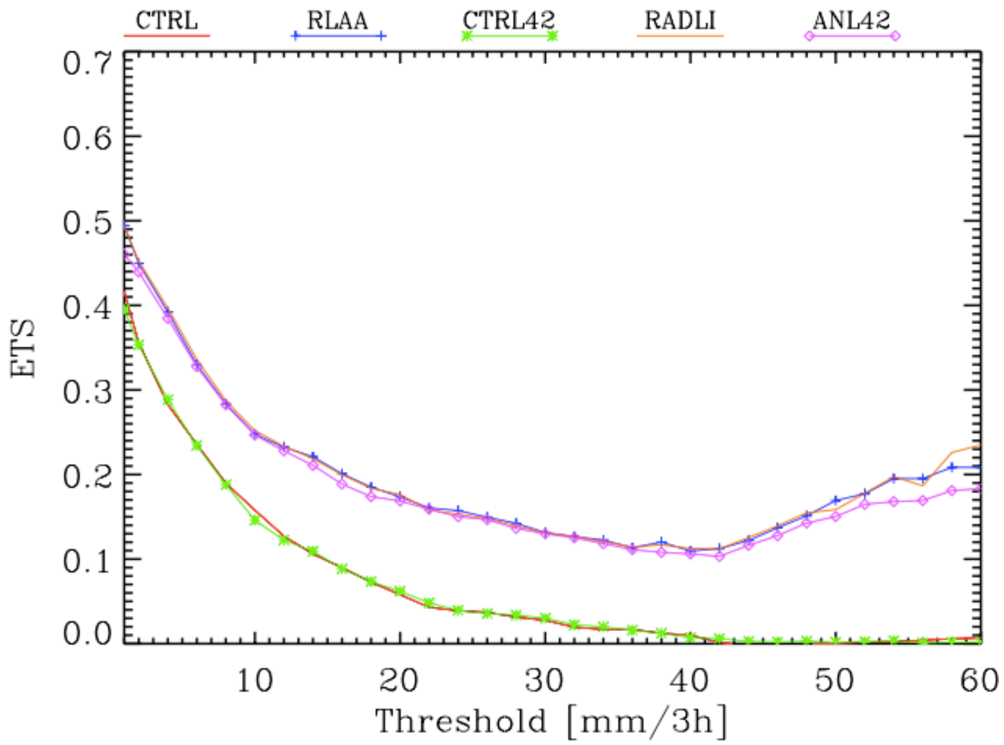

Figure S5: a) POD score for Livorno; b) as in a) for the ETS score. CTRL is the control simulation, RLAA is the simulations with updated IC/BC, CTRL42 is the control simulation using 42 model vertical level, ANL42 is the simulation assimilating radar reflectivity factor and lightning and using 42 model vertical levels. Scores are computed for R4 domain considering all the ten VSF of the Livorno case. Scores are computed for the nearest neighbourhood and for the thresholds: 1mm/3h, 2mm/3h and then every 2 mm/3h up to 60 mm/3h.

a)

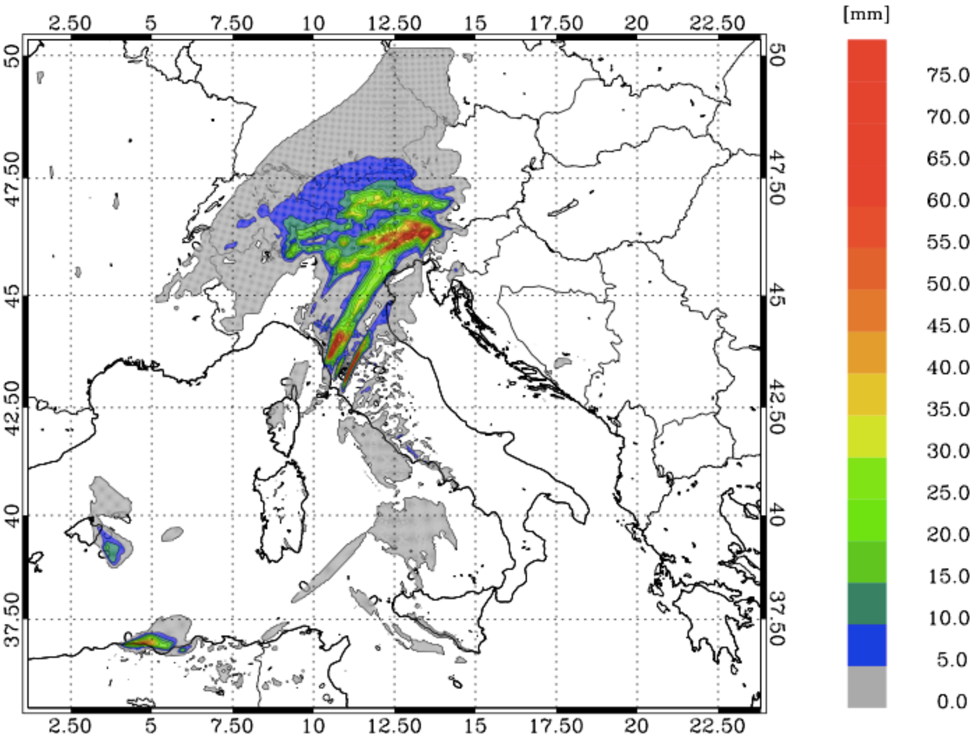
[mm]
75.0
70.0
65.0
60.0
55.0
50.0
45.0
40.0
35.0
30.0
25.0
20.0
15.0
10.0
5.0
0.0
2.50
5
7.50
10
12.50
15
17.50
20
22.50
50
47.50
45
42.50
40
37.50

b)

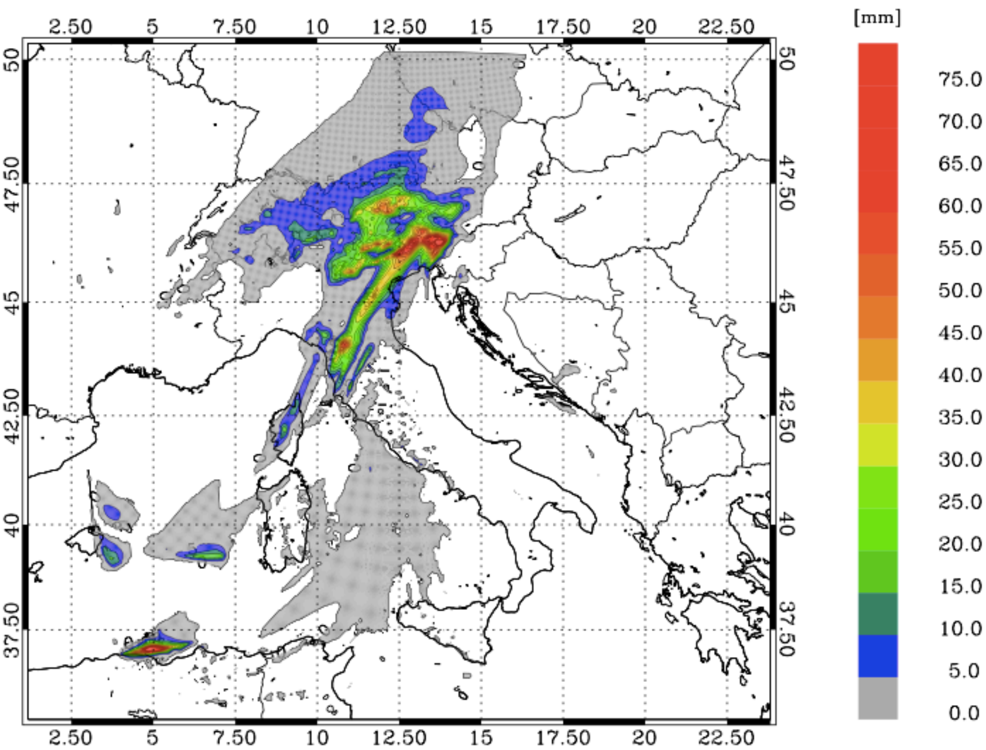
[mm]
75.0
70.0
65.0
60.0
55.0
50.0
45.0
40.0
35.0
30.0
25.0
20.0
15.0
10.0
5.0
0.0
2.50
5
7.50
10
12.50
15
17.50
20
22.50
50
47.50
45
42.50
40
37.50

c)

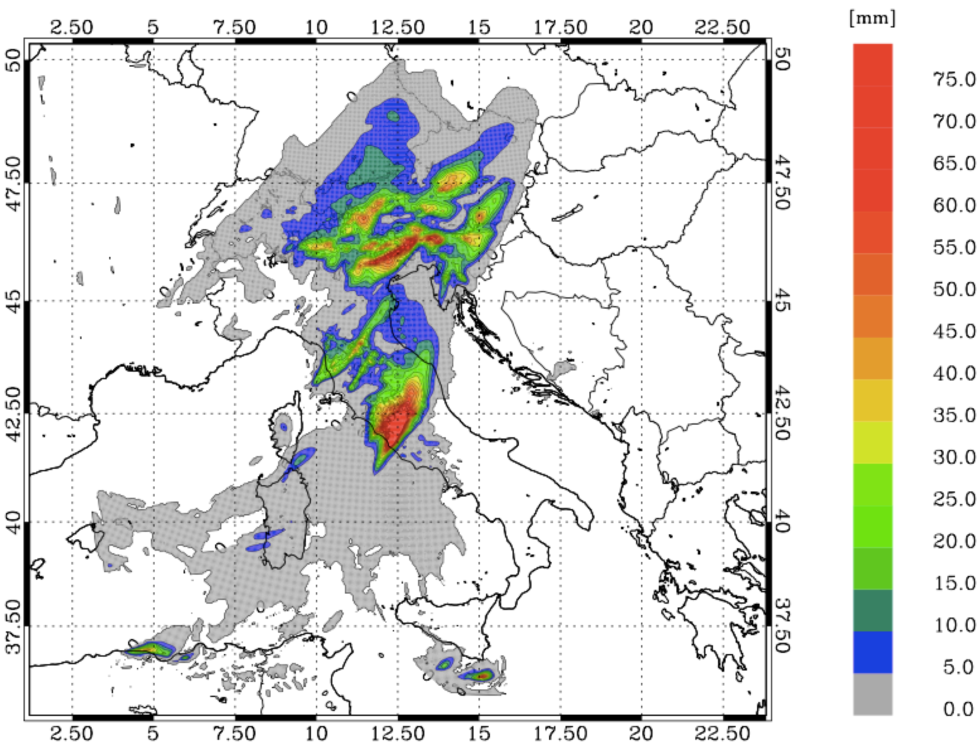

d)

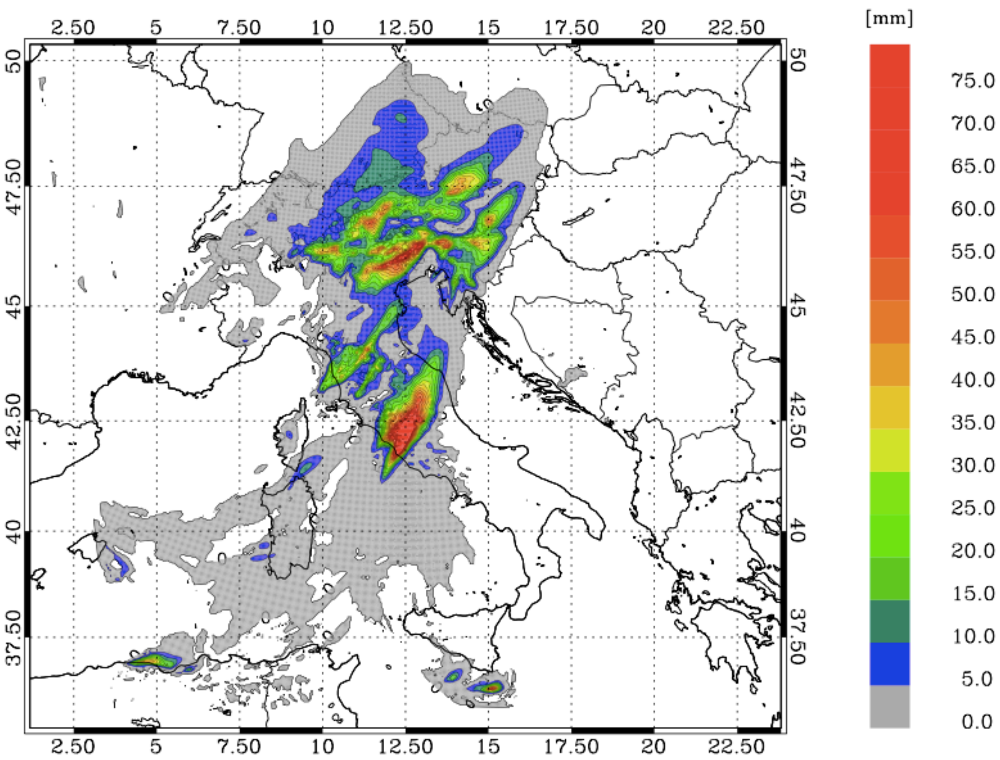

Figure S6: rainfall VSF between 06 and 09 UTC on 10 September for CTRL; b) as in a) for CTRL42; c) as in a) for RADLI; d) as in a) for ANL42.

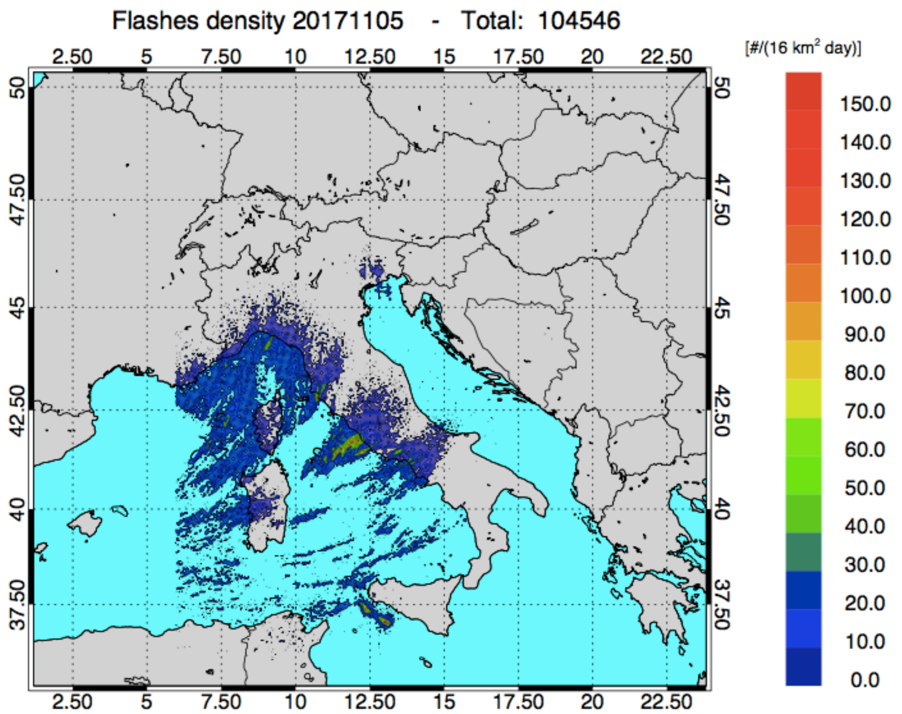

Figure S7: a) Lightning density (lightning number per 16 km^2 for the whole day) recorded on 05 November 2017. The total number of flashes is shown in the title.

a)

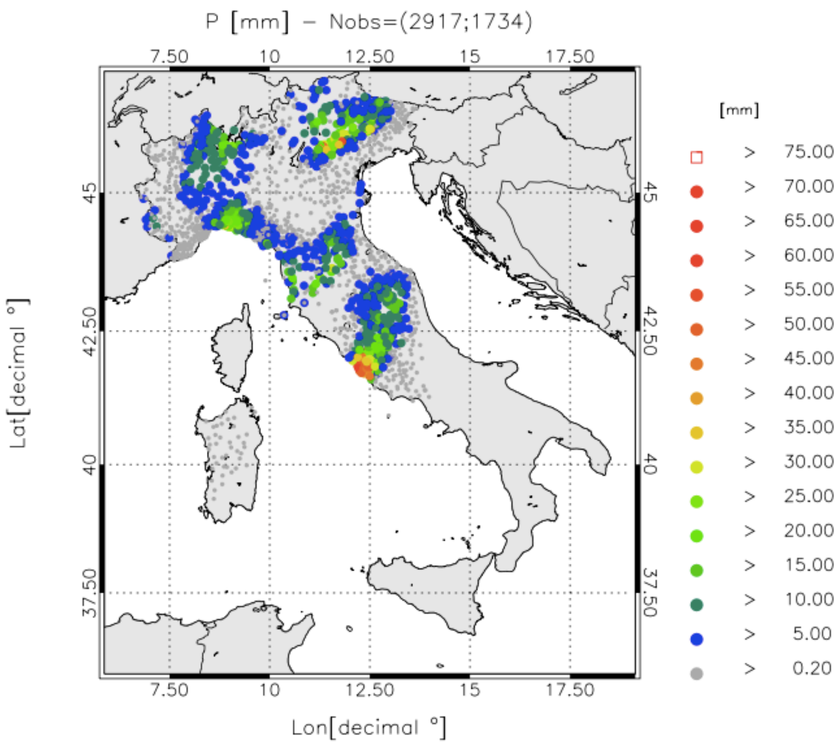

b)

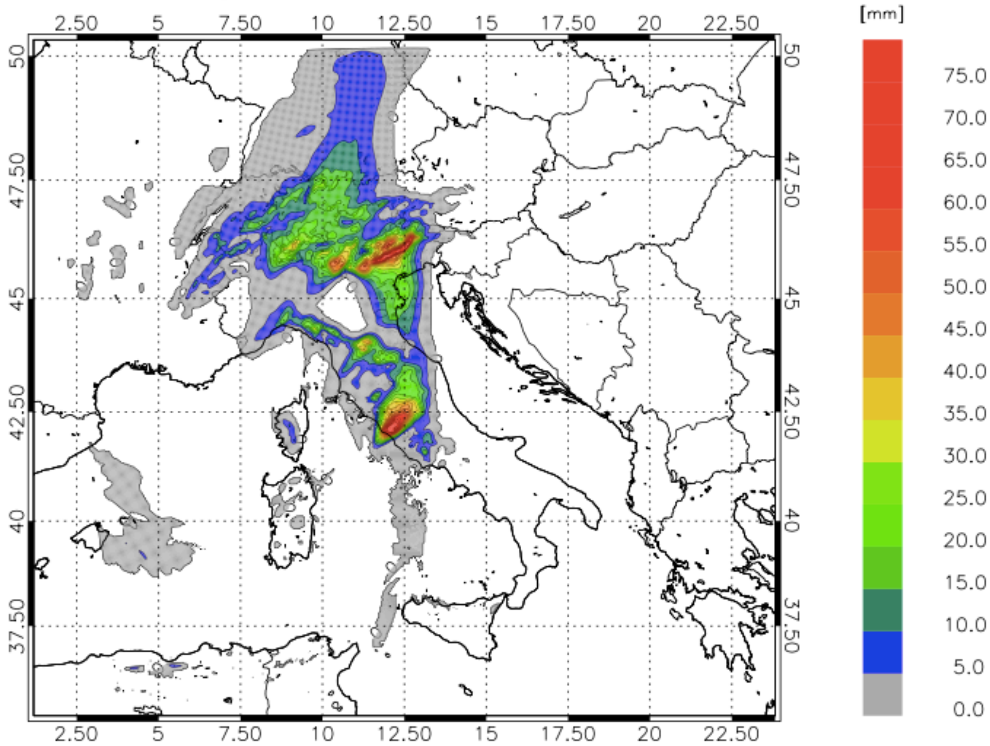

c)

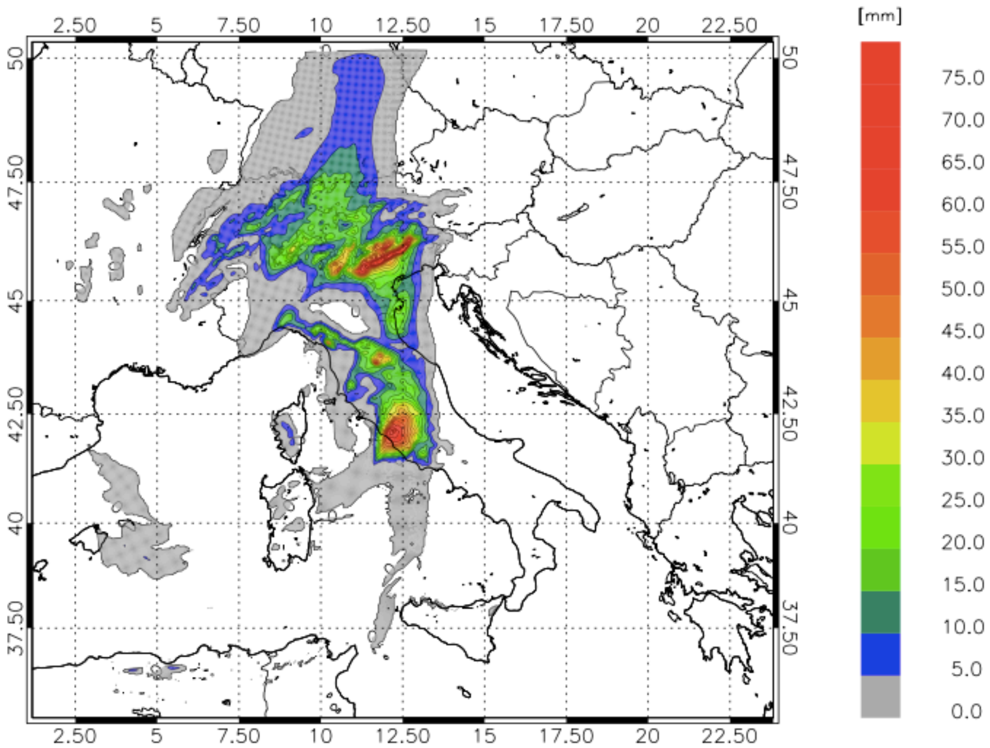

Figure S8: a) rainfall reported by raingauges between 12 and 15 UTC on 5 November 2017. Only stations reporting at least 0.2 mm/3h are shown. The first number in the title within brackets represents the number of raingauges available over the domain, while the second number shows those observing at least 0.2 mm/3h; b) rainfall VSF of CTRL for the same time interval as in a); c) as in b) for LIGHT forecast.

a)

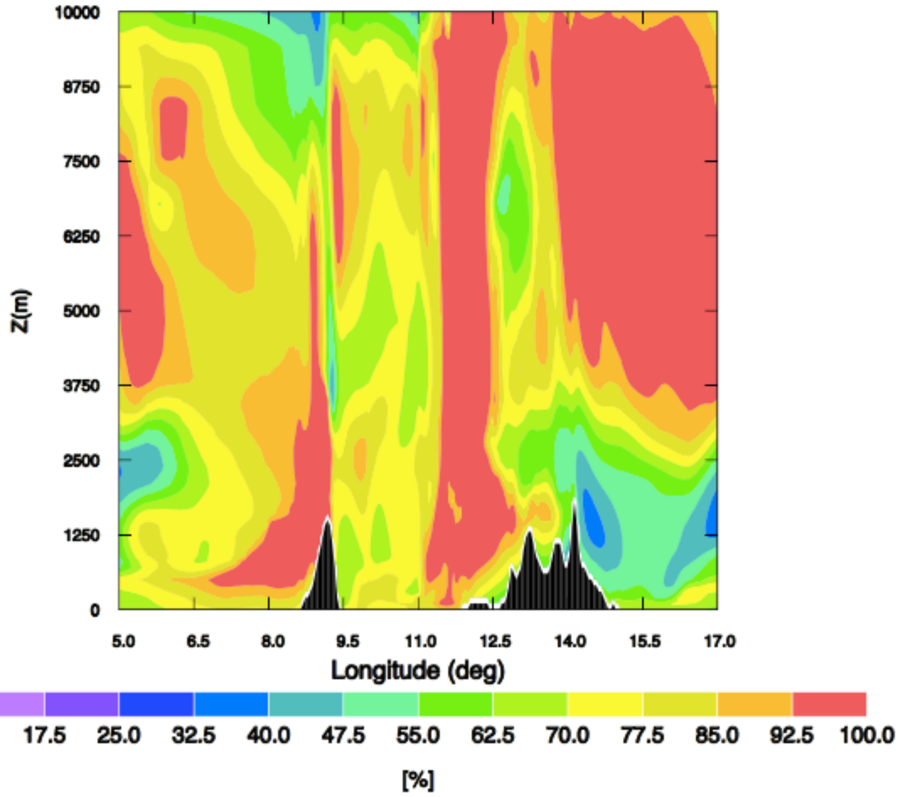

10000
8750
7500
6250
5000
3750
2500
1250
0
Z(m)
5.0
6.5
8.0
9.5
11.0
12.5
14.0
15.5
17.0
Longitude (deg)
10.0
17.5
25.0
32.5
40.0
47.5
55.0
62.5
70.0
77.5
85.0
92.5
100.0
[%]

b)

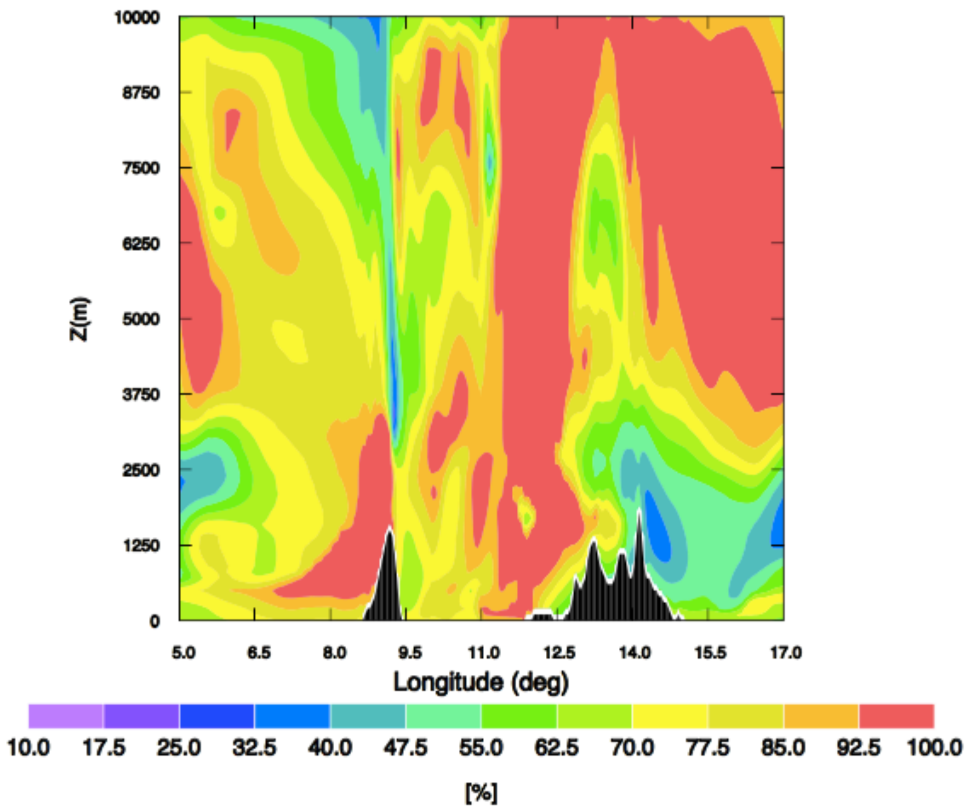

Figure S9: a) Relative humidity longitude-height cross-section at 42°N and at the end of the assimilation period (12 UTC on 5 November 2017) for the CTRL simulation; b) as in a) for LIGHT simulation. Only longitudes between 5 E and 17 E and altitudes between 0 km and 10 km are shown for clarity.

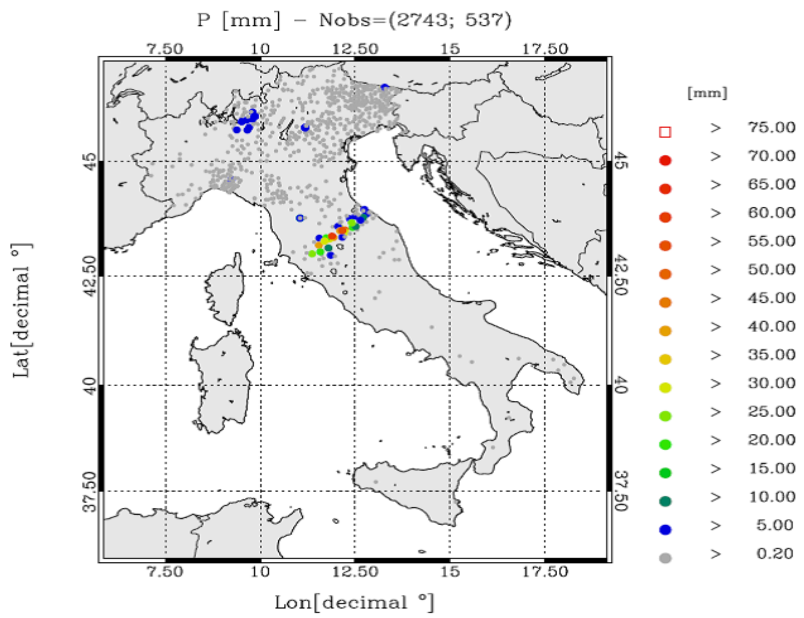

b)

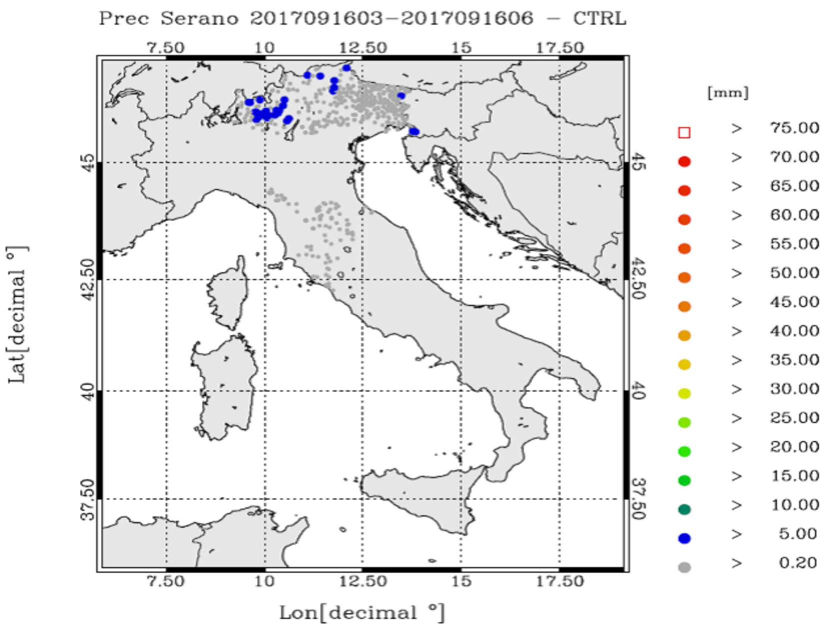
Prec Serano 2017091603–2017091606 – CTRL
7.50
10
12.50
15
17.50
45
42.50
40
37.50
Lat[decimal °]
Lon[decimal °]
[mm]
> 75.00
> 70.00
> 65.00
> 60.00
> 55.00
> 50.00
> 45.00
> 40.00
> 35.00
> 30.00
> 25.00
> 20.00
> 15.00
> 10.00
> 5.00
> 0.20

c)

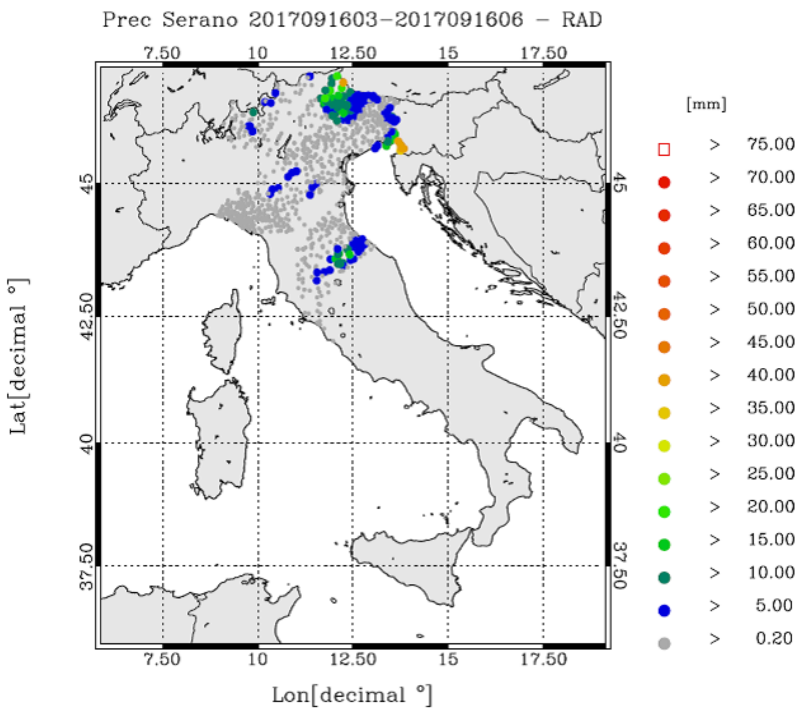
Prec Serano 2017091603–2017091606 – RAD
7.50
10
12.50
15
17.50
45
42.50
40
37.50
Lat[decimal °]
Lon[decimal °]
[mm]
> 75.00
> 70.00
> 65.00
> 60.00
> 55.00
> 50.00
> 45.00
> 40.00
> 35.00
> 30.00
> 25.00
> 20.00
> 15.00
> 10.00
> 5.00
> 0.20

d)

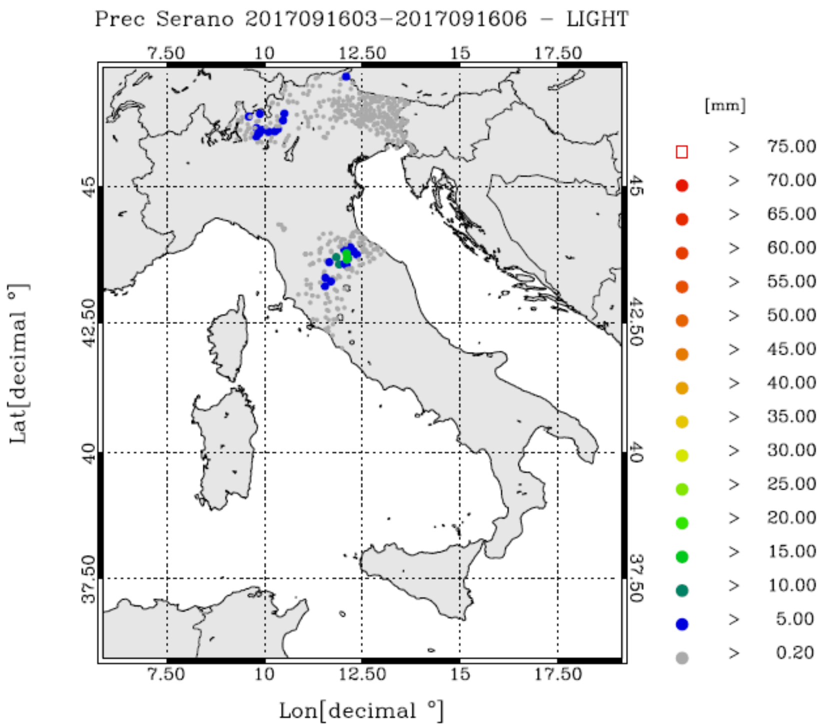

e)

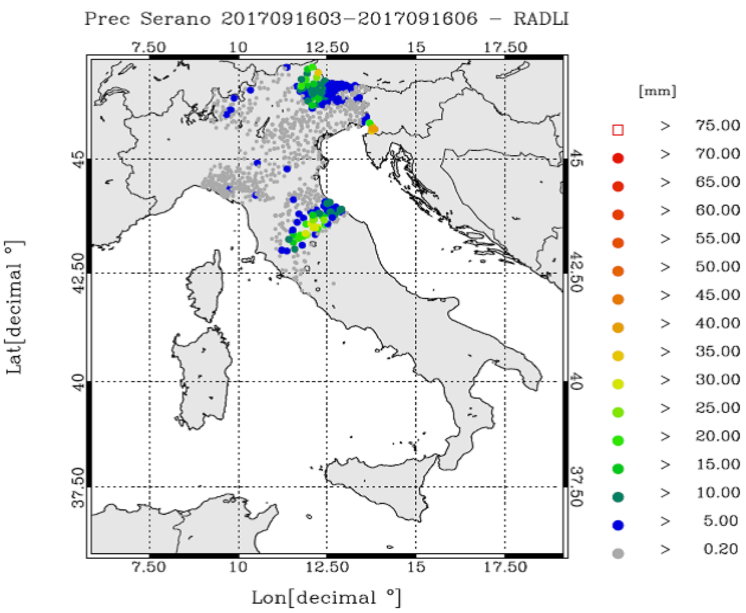

Figure S10: a) rainfall reported by raingauges between 03 and 06 UTC on 16 September 2017. Only raingauges observing at least 0.2 mm/3h are shown. The first number in the title within brackets represents the available raingauges, while the second number represents those observing at least 0.2 mm/3h; b) as in a) for CTRL forecast; c) as in a) for RAD forecast; d) as in a) for LIGHT forecast; e) as in a) for RADLI forecast.

a)

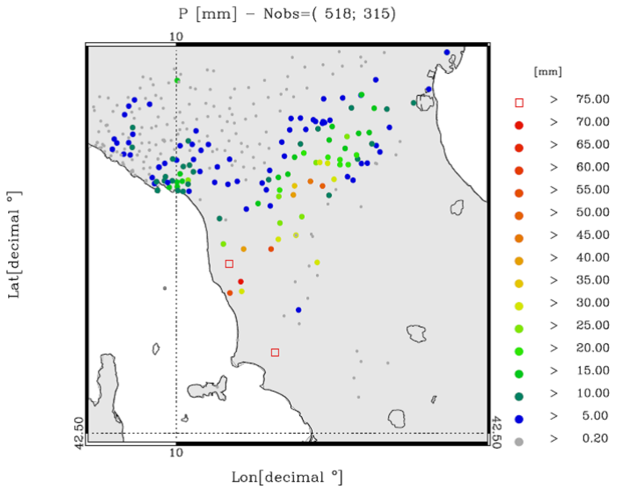

b)

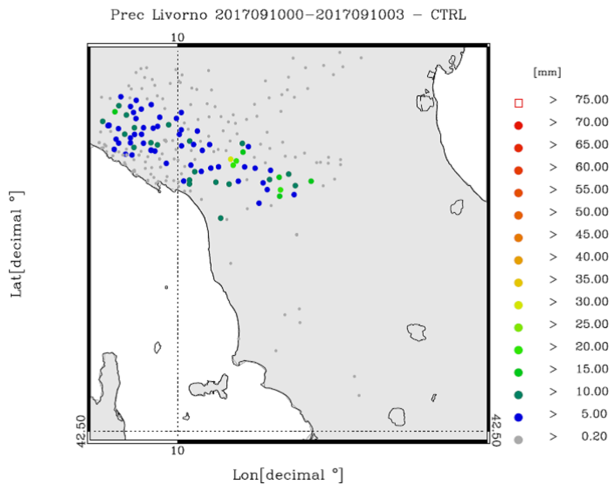

c)

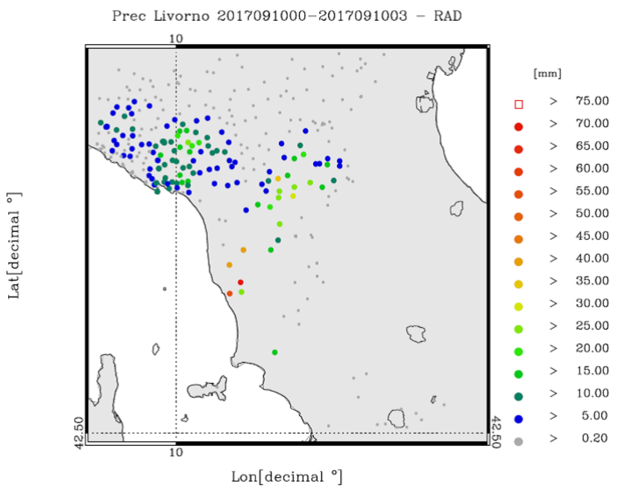

d)

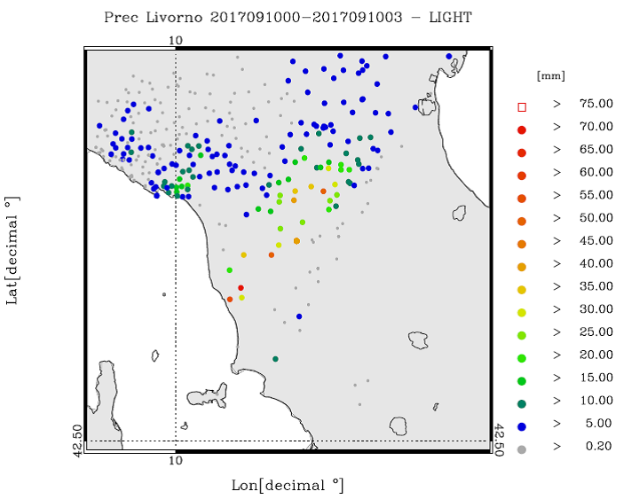

e)

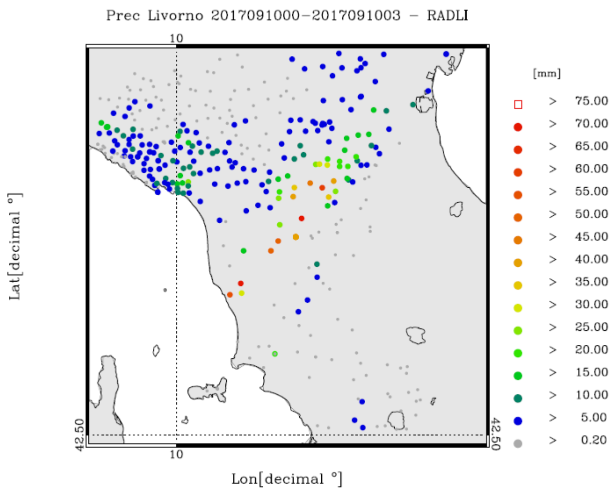

Figure S11: a) rainfall reported by raingauges between 00 and 03 UTC on 10 September 2017. Only stations reporting at least 0.2 mm/3h are shown. The first number in the title within brackets represents the number of raingauges available over the domain, while the second number shows those observing at least 0.2 mm/3h; b) as in a) for CTRL forecast; c) as in a) for RAD forecast; d) as in a) for LIGHT forecast; e) as in a) for RADLI forecast.

a)

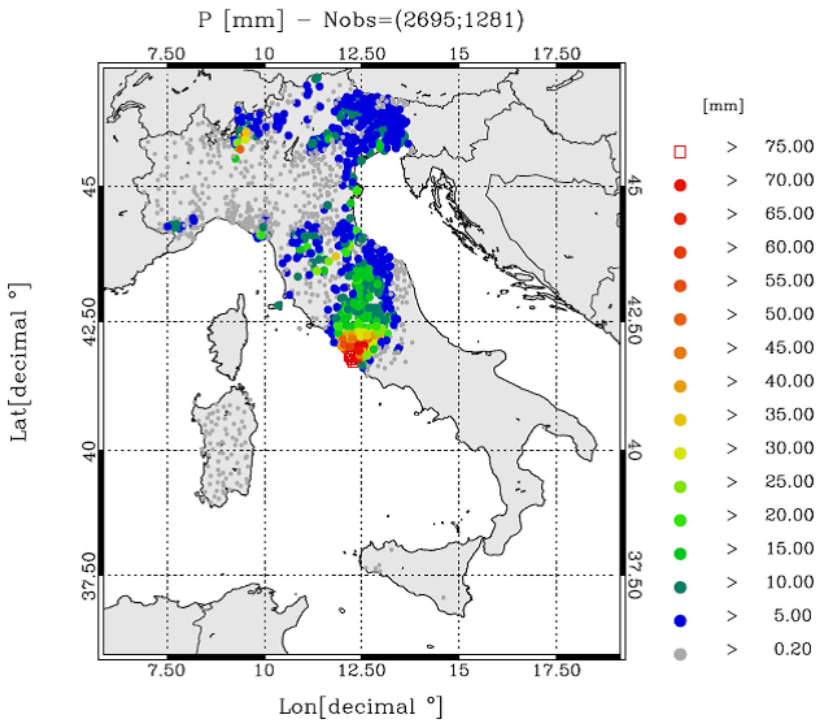
P [mm] – Nobs=(2695;1281)
7.50
10
12.50
15
17.50
45
42.50
40
37.50
Lat[decimal °]
Lon[decimal °]
[mm]
> 75.00
> 70.00
> 65.00
> 60.00
> 55.00
> 50.00
> 45.00
> 40.00
> 35.00
> 30.00
> 25.00
> 20.00
> 15.00
> 10.00
> 5.00
> 0.20

b)

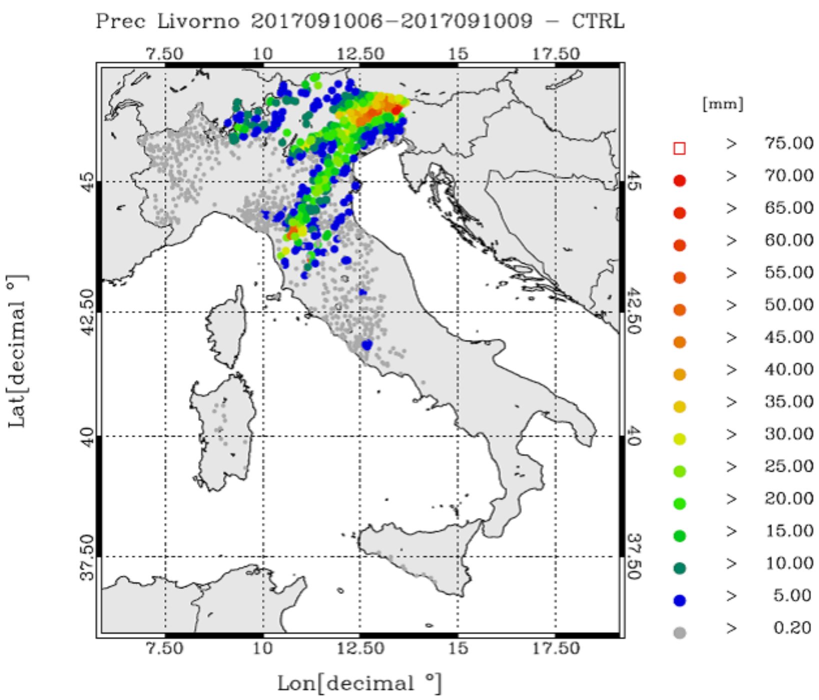
Prec Livorno 2017091006–2017091009 – CTRL
7.50
10
12.50
15
17.50
45
42.50
40
37.50
Lat[decimal °]
Lon[decimal °]
[mm]
> 75.00
> 70.00
> 65.00
> 60.00
> 55.00
> 50.00
> 45.00
> 40.00
> 35.00
> 30.00
> 25.00
> 20.00
> 15.00
> 10.00
> 5.00
> 0.20

c)

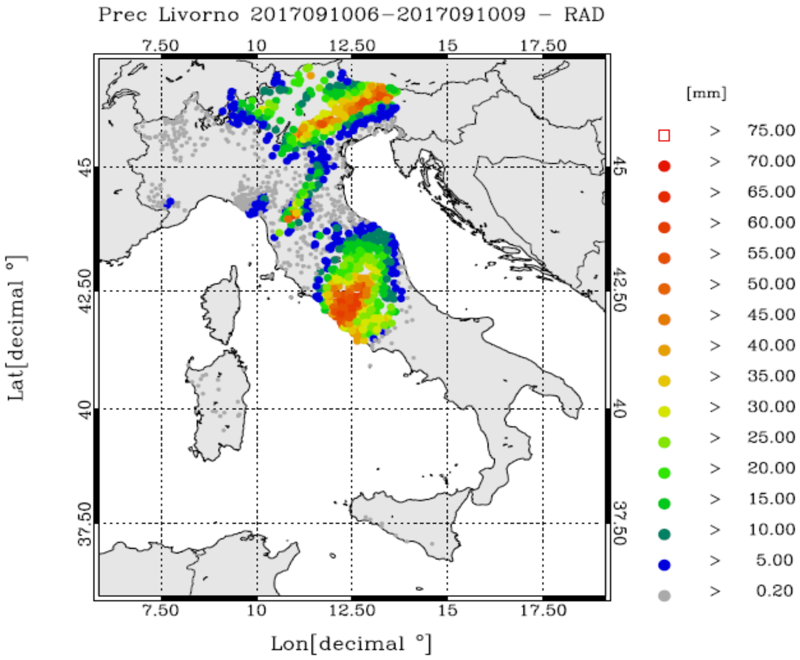
Prec Livorno 2017091006−2017091009 − RAD
Lat[decimal °]
Lon[decimal °]
7.50
10
12.50
15
17.50
45
42.50
40
37.50
[mm]
> 75.00
> 70.00
> 65.00
> 60.00
> 55.00
> 50.00
> 45.00
> 40.00
> 35.00
> 30.00
> 25.00
> 20.00
> 15.00
> 10.00
> 5.00
> 0.20

d)

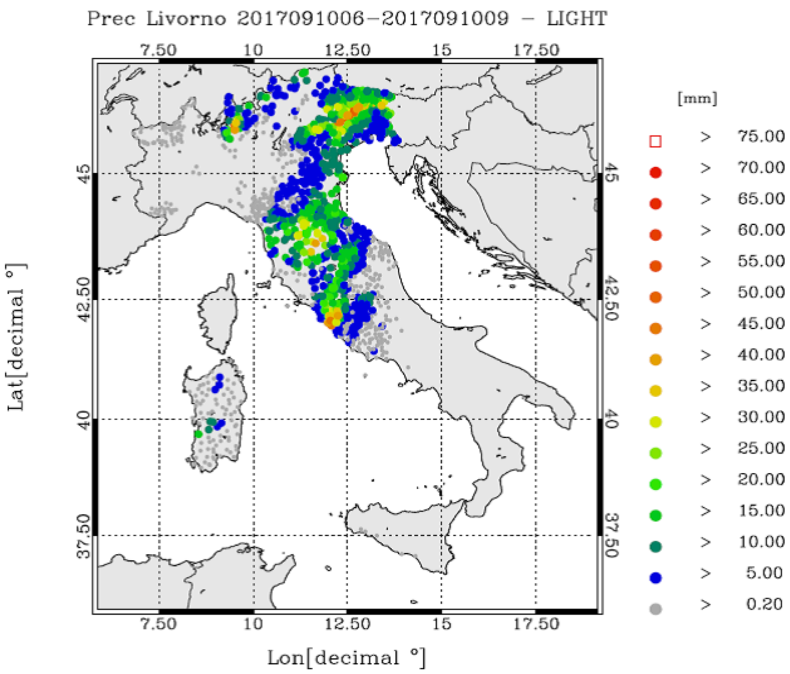
Prec Livorno 2017091006−2017091009 − LIGHT
Lat[decimal °]
Lon[decimal °]
7.50
10
12.50
15
17.50
45
42.50
40
37.50
[mm]
> 75.00
> 70.00
> 65.00
> 60.00
> 55.00
> 50.00
> 45.00
> 40.00
> 35.00
> 30.00
> 25.00
> 20.00
> 15.00
> 10.00
> 5.00
> 0.20

e)

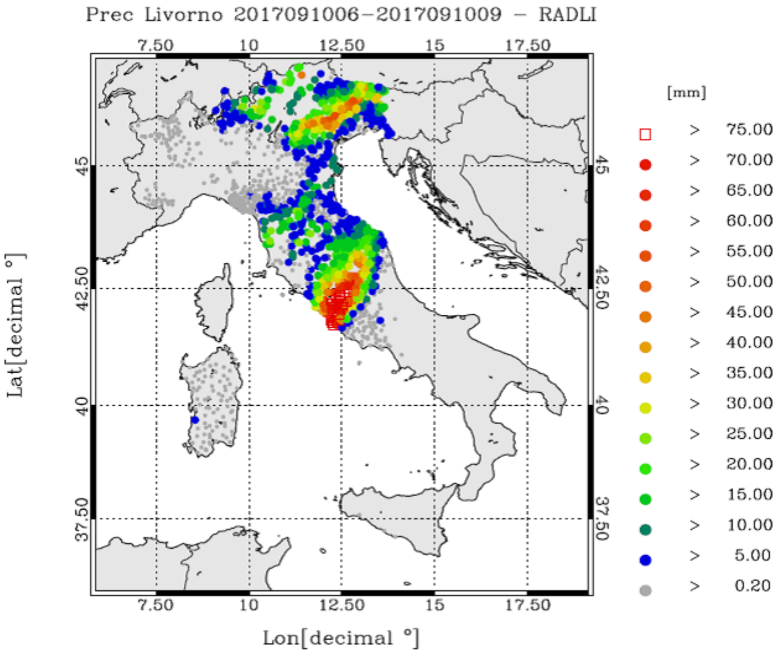

Figure S12: a) rainfall reported by raingauges between 06 and 09 UTC on 10 September 2017. For this time period 2695 raingauges reported valid observations in the domain, however only stations reporting at least 0.2 mm/3h are shown. The first number in the title within brackets represents the number of raingauges available over the domain, while the second number shows those observing at least 0.2 mm/3h; b) as in a) for CTRL forecast; c) as in a) for RAD forecast; d) as in a) for LIGHT forecast; g) as in a) for RADLI forecast.